Keratin 16 Expression Defines a Subset of Epithelial Cells During Skin Morphogenesis and the Hair Cycle

Kelsie M. Bernot, Pierre A. Coulombe, and Kevin M. McGowan

Departments of Biological Chemistry and Dermatology, The Johns Hopkins University School of Medicine, Baltimore, Maryland, U.S.A.

The morphogenesis of skin epithelia and adult hair follicle cycling both require integrated signaling between the epithelium and underlying mesenchyme. Because of their unique regulation, keratin intermediate filaments represent useful markers for the analysis of determination and differentiation processes in complex epithelia, such as the skin. In this study, we analyzed the distribution of mouse type I keratin 16 during skin morphogenesis, in the adult hair cycle, and in challenged epidermis. In mature hair follicles, we find keratin 16 along with its type II keratin partner keratin 6 in the companion layer of the outer root sheath during anagen and in the club hair sheath during catagen and telogen. During embryonic development, the distribution of keratin 16 is uncoupled from its presumed polymerization partner, keratin 6. Keratin 16 initially localizes within early hair germs, but rapidly shifts to a subset of cells at the interface of basal and suprabasal cells above and around the hair germ. The presence of keratin 16 at the transition between mitotically active and differentiating cells is recapitulated in primary keratinocytes cultured *in vitro* and in phorbol 12-myristate 13-acetate-treated back skin *in vivo*. We propose that keratin 16 marks cells in an intermediate state of cellular properties in which keratinocytes retain the flexibility required for activities such as cell migration and even mitosis but are resilient enough to provide the structural integrity required of the early suprabasal layers in the context of development, adult hair cycling, and wound repair. ***Key words: epidermis/hair follicle/intermediate filament/sweat gland/wound healing. J Invest Dermatol 119:1137–1149, 2002***

The morphogenesis of skin epithelia requires complex signaling interactions between the embryonic ectoderm and mesoderm (Sengel, 1983; Hardy, 1992). Onset of differentiation within the mouse ectoderm begins at embryonic day 9.5 (e9.5) (Byrne *et al*, 1994). Specification towards an appendageal fate, hair in particular, occurs concomitant with onset of stratification at e10.5–e11 (Sanes *et al*, 1986; Kopan and Fuchs, 1989; Byrne *et al*, 1994; McGowan and Coulombe, 1998a). Hair morphogenesis progresses in a synchronized wave along the anterior-to-posterior and also dorsal-to-ventral axes of the embryo (Mann, 1962). Although the epidermis becomes fully differentiated and acquires adult-like barrier properties at about e16.5, the hair follicles will continue to elongate and differentiate past birth (Greer and Roop, 1991; Byrne *et al*, 1994; Hardman *et al*, 1998).

Growth of the hair follicle does not end with full maturation of the animal; in fact, the hair cycles through periods of growth (anagen), regression (catagen), and rest (telogen) (Dry, 1926; Chase *et al*, 1951). During anagen, the follicle proliferates deep into the hypodermis of the skin, and the hair shaft actively grows in length. During the first two hair cycles in rodents, induction of catagen occurs as a wave along the anterior-to-posterior axis (Chase and Eaton, 1959), just as in hair morphogenesis. Whereas cells in the lower part of the follicle undergo a massive wave of apoptosis (Weedon and Strutton, 1981), the regressing follicle maintains its attachment to the hair shaft via the club hair sheath (CHS) (Lavker *et al*, 1998). To allow for maintenance of a full hair coat, the club hair remains attached to the follicle through both telogen and induction of the next anagen phase (Chase and Eaton, 1959). The hair follicle continues to cycle for most of the life of the animal, although for mice synchronization is lost after the second cycle.

Because of their regulation in a pairwise, epithelial tissue-type, and differentiation-specific manner, keratins are useful tools for studying epithelial differentiation (Moll *et al*, 1982; O'Guin *et al*, 1990; Coulombe and McGowan, 2000). Type I and type II keratin proteins are encoded by a multigene family (>25 members each) and obligatorily heteropolymerize with one another to produce intermediate-sized filaments in the cytoplasm of epithelial cells (Hesse *et al*, 2000; Coulombe *et al*, 2001). Type I keratins (K9–K21; Ha1–Ha8) range from 40 to 63 kDa and are more acidic, whereas type II keratins (K1–K8; Hb1–Hb6) are larger (53–67 kDa) and more basic (Moll *et al*, 1982). Keratin filament networks generally function as a structural scaffold, providing mechanical support not only for individual cells, but also for an entire epithelial sheet. Evidence for this function comes from the discovery of keratin mutations that cause skin blistering diseases, coupled with the existence of phenocopies of such diseases in mice transgenic for mutant keratins (Fuchs and Cleveland, 1998; Coulombe and Omary, 2002). Consistent with the large number and restricted distribution of these keratin proteins, additional functions manifested in a sequence- and context-specific fashion have recently been uncovered (Coulombe and Omary, 2002).

Initially during development, the single-layered embryonic ectoderm expresses the K8–K18 pair, which is characteristic of adult

Manuscript received June 29, 2002; revised July 30, 2002; accepted for publication August 5, 2002

Reprint requests to: Pierre A. Coulombe, Department of Biological Chemistry, Johns Hopkins University School of Medicine, 725 N. Wolfe Street, Baltimore, MD 21205; Email: coulombe@jhmi.edu

Abbreviations: CHS, club hair sheath; e, embryonic day; K. keratin; ORS, outer root sheath

simple epithelia. Expression of the K5 and K14 gene occurs at e9.5 in this layer, before the onset of stratification and differentiation (Byrne *et al*, 1994). Shortly thereafter, onset of K17 expression occurs in a subset of ectodermal cells in the context of epithelial–mesenchymal interactions, reflecting the adoption of a nonepidermal cell fate (McGowan and Coulombe, 1998a). K17, along with K6 and K16, is expressed constitutively in epithelial appendages and is induced strongly in response to injury and other acute challenges in adult complex epithelia.

A growing body of evidence suggests that K16 exhibits special properties that may translate into a specialized function(s) in keratinocytes. Although K16 and K14 are highly homologous in primary structure, targeted expression of K16 to the basal layer of the epidermis only partially rescues the severe skin phenotype and early death of the K14 null mice; these replacement mice develop late-onset blistering disease and alopecia (Paladini and Coulombe, 1999). Biophysical studies demonstrate that K5/K16 polymers exhibit weaker micromechanical properties than K5/K14 polymers under conditions promoting keratin filament bundling *in vitro* (Yamada *et al*, 2002). Moreover, modest overexpression of K16 in transgenic mice partially impairs the epithelialization of skin wounds *in vivo* and *ex vivo* (Wawersik *et al*, 2001). Studies on keratinocytes cultured from these same mice reveal that K16 effects changes in the cytoplasmic organization of keratin filaments and in cell adhesion in a context-dependent fashion (Paladini and Coulombe, 1998; Wawersik and Coulombe, 2000; see also Porter *et al*, 1998). K16 expression has also been implicated in cell cycle control (Paramio *et al*, 1999), although the mechanistic basis for this has been disputed (Paladini and Coulombe, 1999). These data, along with other work (Swensson *et al*, 1998), imply that K16 imparts distinct properties to keratinocytes in which it is expressed. The importance of K16, along with K6 and K17, in biological processes such as wound healing prompted us to undertake the analysis of K16 expression during mouse embryonic and postnatal development of skin epithelia, and relate its expression to that of its presumed type II polymerization partner K6 as well as the related type I keratins K14 and K17.

MATERIALS AND METHODS

Materials Materials were obtained from the following sources: 129SvJ mouse genomic library packaged into Lambda Fix II and pBluescript vector, Stratagene (LaJolla, CA); restriction endonucleases, New England Biolabs (Beverly, MA); Superscript II reverse transcriptase, Life Technologies (Grand Island, NY); Nytran membranes, Schleicher and Schuell (Keane, NH); Hybond-N filters and Immobiline DryStrip Gel pH 4.0–7.0, Amersham Pharmacia Biotech (Piscataway, NJ); DNA purification kits, Qiagen (Santa Clarita, CA); LA-Taq DNA polymerase, Panvera (Madison, WI); Protean II Ready Gel Precast 10% Acrylimide Gel, Bio-Rad (Hercules, CA); phorbol 12-myristate 13-acetate (PMA), Sigma (St. Louis, MO); all-*trans*-retinoic acid, Nacalai Tesque (Japan). All other chemicals were reagent grade and typically obtained from Sigma.

Animal protocols All studies involving animals were reviewed by the Johns Hopkins University Animal Use and Care Committee. For isolation of RNA from wounded back skin, 129SvJ adult mice (Jackson Laboratory, Bar Harbor, ME) were anesthetized with avertin, and their backs were depilated with Nair cream (Carter-Wallace, New York, NY). After disinfection, full-thickness skin wounds were made with a scalpel. For histological analysis of wounded back skin, 5-d-old pups were treated in the same manner as above, except the hair was not removed. After cervical dislocation, wound edge tissue was dissected and frozen in liquid nitrogen. Chemical induction of K16 was achieved by topical application of PMA or all-*trans*-retinoic acid. For PMA, 100 μl of a 50 μM stock of PMA in acetone was applied three times on an every other day basis, and the skin was harvested on the seventh day. For all-*trans*-retinoic acid, 100 μl of 100 μg per ml stock of all-*trans*-retinoic acid in ethanol was applied six times on an every other day basis prior to harvesting the tissue. For developmental studies, timed pregnancies of B6C3F1/J mice were set up, using 12:00 noon the morning after overnight mating as e0.5 (Kaufman, 1992). Pregnant female mice were euthanized by ether vapor exposure at noon various days after mating (J.T. Baker, Mallinckrodt Baker, Phillipsburg, NJ), and embryos were isolated. All tissue was processed in one of two ways: (i) frozen immediately without fixation in Optimal Cutting Temperature (OCT) compound (Tissue-Tek, Sakura Finetek, Torrance, CA) followed by sectioning (10 μm); or (ii) fixed in Bouin's fixative overnight at 4°C and then embedded in paraffin and sectioned (5 μm). Standard indirect immunohistochemistry protocols were followed (Takahashi *et al*, 1994). Bound antibody was detected by a peroxidase-based reaction or via indirect immunofluorescence.

Screening the mouse genomic library The strategy applied for the screening of the 129SvJ mouse genomic library for epidermal type I keratin genes has been described previously (McGowan and Coulombe, 1998a). Approximately 1.5×10^6 phage clones were screened with [^{32}P]dCTP radiolabeled probes derived from the rod portion of the human keratin 16 cDNA (Paladini *et al*, 1995) or the 3′ end of the mouse K17 cDNA (McGowan and Coulombe, 1998a). Positive colonies were isolated by repeated plaque purification as described previously (Sambrook *et al*, 1989). DNA fragments were subcloned into pBluescript KS+. DNA sequencing and reconstruction of mouse K17/K16 locus was performed with the assistance of the JHU DNA Sequencing Core Facility.

RNA isolation and cDNA cloning Total RNA was extracted from various tissues including control and wounded back skin using the GTC-phenol extraction method (Bessho *et al*, 1993) as described previously (McGowan and Coulombe, 1998a). A cDNA clone containing the entire coding sequence of K16 was obtained via reverse transcription polymerase chain reaction (RT-PCR) using total RNA extracts. Primers used were as follows: forward, 5′-TGCTCACTTGCCCACACTCTCCAGTTCCT-CACCATGGCCACC-3′; reverse, 5′-GCCTACCACCATGAGAGGG-TAGGGGAGACAGA TGGGGAATGCGCA-3′. The resulting 1.3 kb PCR product was subcloned into the vector pGEM-T-Easy (Promega, Madison, WI) and subjected to sequencing analysis. To facilitate subsequent subcloning steps, the forward primer contained a single base mismatch creating a restriction endonuclease Nco I site (underlined in sequence). The PCR conditions were 94°C for 1 min (denaturation), 55°C for 1 min (annealing), and 72°C for 2 min (elongation), for 25 cycles.

Differential splicing analysis PCR primers were used to amplify a 474/477 bp fragment from the K16 cDNA 3′ end: forward primer, 5′-AACAG-CCTAGAAGAGACCAAAGGC-3′, the 5′ end of which is located 206 bp upstream of the alternative splice site; reverse primer, same as above. Digestion of the PCR products with Alu I produces distinct fragments of either 221 bp for K16b (3 serine isoform) or 119/105 for K16a (4 serine isoform). Individual bands were visualized by electrophoresis on a 3% agarose gel. These primers were also applied to a mouse genomic DNA template, which produced a single 695 bp product as verified by subcloning and sequencing 10 isolates. The PCR conditions applied were the same as above.

Transient expression of mK16 in cultured cells *in vitro*, production of recombinant protein in *Escherichia coli*, and filament assembly The complete cDNAs encoding the K16a (4 serine) and K16b (3 serine) isoforms were subcloned into the vector pBK-CMV (Stratagene). Transient expression and immunostaining of cell cultures were performed as previously described (Paladini *et al*, 1996) using PtK2 cells, a kangaroo kidney epithelial cell line (American Type Culture Collection, Rockville, MD). To produce recombinant mouse K16 proteins, K16a or K16b cDNAs were subcloned into the expression vector pET-3d. The pET-mK16 and pET-mK6β (Takahashi *et al*, 1998) constructs were transformed into the BL21 (DE3) strain of *E. coli* for T7 RNA polymerase-based expression as described previously (Coulombe and Fuchs, 1990). After solubilization in a 6.5 M urea-containing Tris–HCl buffer, the protein was purified to near homogeneity by ion-exchange chromatography on a Hi-Trap Q column followed by a Mono Q column as described previously (Wawersik *et al*, 1997). Purified recombinant type I and type II keratins were mixed at a 200 μg per ml protein concentration, incubated for 1 h at room temperature, and fractionated by anion-exchange chromatography on a Mono Q column as described above. Collected fractions (0.5 ml) were analyzed by sodium dodecyl sulfate polyacrylamide gel electrophoresis (SDS-PAGE), and fractions containing type I–type II heterotypic complexes in a 1 : 1 molar ratio were pooled. Keratin protein concentration was fixed at 0.25 mg per ml (≈4 μM). Renaturation and polymerization of keratins was achieved by serial dialysis against the following three buffers at room temperature: (i) 9 M urea, 25 mM Tris–HCl, 10 mM β-mercaptoethanol, pH 7.4, for at least 4 h; (ii) 4 M urea, 5 mM Tris–HCl, 5 mM β-mercaptoethanol, pH 7.4, for 1 h; (iii) 5 mM Tris–HCl, 5 mM β-mercaptoethanol, pH 7.4, overnight. Keratin filament preparations were examined by negative staining (aqueous 1% uranyl acetate) and electron microscopy (Zeiss 10 A, Carl Zeiss, Germany) as described previously (Coulombe and Fuchs, 1990).

Two-dimensional gel electrophoresis Pelage mouse hair clippings were minced, and keratins were extracted as described previously (McGowan and Coulombe, 2000). Protein extract, 30 μg, was separated by isoelectric focusing on an Immobiline DryStrip Gel pH 4.0–7.0. The isoelectric focusing strip was then run onto a precast denaturing 10% polyacrylamide gel (Bio-Rad) in order to separate proteins by molecular weight. The two-dimensional gel was then electroblotted onto nitrocellulose and probed with antibodies to detect K16 and acidic hair keratins.

Primary keratinocyte culture Primary keratinocytes were isolated from wild-type 3–5-d-old pups of the B6C3F2 mixed background as described previously (Rhouabhia *et al*, 1992). Final cell pellets were resuspended in calcium-free minimum essential medium (Biowhittaker, Walkerville, MD), 8% Chelex-treated fetal bovine serum (Intergen, Purchase, NY), 50 units per l Pen-Strep (Mediatech, Herndon, VA), and 0.12 mM calcium. Cells were plated onto coverslips at a density of approximately 2×10^5 cells per 35 mm well and grown overnight. Cells were then washed with calcium-free phosphate-buffered saline (PBS) and grown in medium containing 0.05 mM ("low") calcium up to 72 h until they reached 95% confluency. After a 2 h pulse treatment with 50 nM 5-bromo-2′-deoxyuridine (BrdU) (Sigma), cells were washed with PBS. The medium was switched to 0.2 mM ("high") calcium, and the cells continued to grow up to 96 h. Coverslips were removed at the end of the BrdU pulse for the 0 h timepoint. Subsequent timepoints were 6, 12, 24, 48, 72, 96 h after the BrdU label. Cells were fixed with 100% methanol at −20°C for 5 min.

Antibodies We developed a polyclonal rabbit antiserum, designated KHmK16, directed against a C-terminal peptide in the mouse K16 protein. The synthetically produced peptide NH2-C-S-T-S-F-S-Q-S-Q-S-Q-S-S-R-D-COOH was conjugated to maleimide-activated keyhole limpet hemocyanin carrier (Pierce Chemical, Rockford, IL). Rabbits were immunized according to standard procedures (Covance Research Products, Denver, PA). To test the antisera, known quantities of K16 recombinant protein were subjected to SDS-PAGE next to extracts from mouse primary keratinocytes, tongue, colon, and normal and wounded back skin. The gel was electroblotted onto nitrocellulose membrane and subjected to Western blotting with one of the following three antibodies: the rabbit polyclonal 1275 (Takahashi *et al*, 1994) or K8.12 (Sigma), which are known to react with K16, or our new KHmK16. Secondary antibodies conjugated to horseradish peroxidase (Sigma) were applied, followed by reagents for enhanced chemiluminescence per the manufacturer's instructions (Pierce). Other primary antibodies used were a rabbit polyclonal against K17 (McGowan and Coulombe, 1998a), a rabbit polyclonal against K6 α and β isoforms (does not recognize K6hf; McGowan and Coulombe, 1998a; Wong *et al*, 2000), and mouse monoclonals LL001 directed against K14 (Purkis *et al*, 1990), K8.60 directed against K1, K10, and K11 (Sigma), K8.12 directed against K13, K15, and K16 (Sigma), and AE13 directed against type I acidic hair keratins (Lynch *et al*, 1986). Other secondary antibodies used were fluorescence-conjugated, goat-produced IgG directed against mouse or rabbit heavy chains (KPL, Gaithersburg, MD). In the case of double labeling with two monoclonal antibodies, after blocking, cells were first reacted with anti-BrdU followed by rhodamine-coupled secondary antimouse. Monoclonal anti-K10 was then followed by fluorescein-isothiocyanate-coupled secondary antimouse. Because of dissociation/reassociation of antibodies during the procedure, some of the fluorescein-isothiocyanate-conjugated secondary bound to the mouse anti-BrdU primary antibody. This results in the appearance of nuclei that are both rhodamine and fluorescein isothiocyanate positive. Because BrdU is present only in the nucleus whereas K10 is cytoplasmic and filamentous, we can easily differentiate between the two antigens, even when the secondary antibody reacts to the "wrong" primary antibody.

RESULTS

Using a probe corresponding to the central rod domain of human K16 (Paladini *et al*, 1995), we screened 1.0×10^6 clones (average insert size 15–20 kb) from a 129SvJ mouse genomic library. Further screening and purification lead to isolation of the K17 gene (McGowan and Coulombe, 1998a). Given the previous demonstration that the functional human K16 gene is located immediately 3′ to the functional human K17 gene (Troyanovsky *et al*, 1992), we postulated that the mouse K16 and K17 genes were organized in the same manner within the type I keratin gene locus. This was indeed the case, and we were able to isolate all exons and introns, 5′ upstream, and 3′ noncoding segments for a candidate K16 genomic clone (GenBank Accession number #AF264006). The boundaries of these functional elements were established via comparison with the cloned human K16 gene (Rosenberg *et al*, 1988) and with mouse K16 cDNA clones. The candidate mouse K16 gene shows a structure that is identical to that shared by all type I keratin genes, including human K16 (Rosenberg *et al*, 1988), with eight exons interrupted by seven introns. Expression of the full-length genomic clone using the CMV promoter in transiently transfected PtK2 cells gives rise to an antigen that is recognized by anti-K16 antibodies and that localizes to the keratin filament network (data not shown). These and other data established that the type I keratin gene isolated is functional and encodes the mouse ortholog of human K16.

Two distinct mouse K16 cDNA clones differ by a single Ser amino acid residue Oligonucleotide primers spanning the putative translation start codon (forward direction) and 3′ nontranslated region (reverse direction) in the candidate K16 gene were used to obtain a ≈1.3 kb cDNA clone by RT-PCR. The yield in PCR product was reproducibly >3-fold higher in wounded skin total RNA compared to intact skin (data not shown). Upon sequencing of several independent subclones, two types of cDNA clones differing by a single extra codon located at the intron 6-exon 7 boundary of the gene could be recognized (**Fig 1*A***). As a result, one of the two mRNA products features an additional serine-encoding codon ("CAG") at the very beginning of the predicted nonhelical tail domain, a sequence context that already features three consecutive serine codons. Inspection of the nucleotide sequence at the intron 6-exon 7 boundary reveals a partial duplication of the consensus splice acceptor site ("AG") at the 3′ end of intron 6 that is consistent with the two products discovered during cDNA cloning (**Fig 1*A***). The two isoforms are designated K16a (4-Ser) and K16b (3-Ser), and are the products of utilization of the 5′- and 3′-most consensus splice acceptor, respectively. There is no duplication of the 3′ splice acceptor site at the intron 6-exon 7 boundary in the human K16 gene (Rosenberg *et al*, 1988).

We developed an RT-PCR-based assay to discriminate between the K16a and K16b mRNA transcripts using restriction enzyme digestion and agarose gel electrophoresis (see *Materials and Methods*). The specificity of the assay for K16a and K16b mRNA transcripts was confirmed using cloned cDNAs (**Fig 1*B***). We applied this assay to RNA samples prepared from a variety of adult mouse tissues known to express K16, including control and wounded back skin, foot pad epidermis, tongue, pancreas, and anal canal. In addition, we tested RNA samples prepared from the back skin of e16.5 and e18.5 mouse embryos. Irrespective of the source, we found a similar ratio between the K16a and K16b transcripts, with a consistent bias towards K16b (**Fig 1*C***). These findings suggest that the differential splicing postulated to occur at the intron 6-exon 7 junction is not subject to tissue-specific regulation and might simply reflect the alternative use of two neighboring acceptor sites on the part of the splicing machinery (Chen *et al*, 2000). The mouse K16 cDNA clone previously reported by Porter *et al* (1998) corresponds to the K16b cDNA clone we report here.

Properties of mouse K16 protein Both mK16a and mK16b cDNA clones were placed in BK-CMV plasmids with their expression driven by the CMV promoter. When each plasmid was transiently transfected into kangaroo kidney epithelial cells (PtK2 cells), the corresponding protein was incorporated into the existing K8/K18 intermediate filament network (**Fig 1*D***). We developed a polyclonal antiserum, termed KHmK16, directed against a C-terminal peptide from the mouse K16 protein. KHmK16 specifically recognized a single band of approximately 50 kDa on a Western blot of keratinocyte extract that migrated at the same position as recombinant mouse K16 protein. This band disappeared when the antiserum was

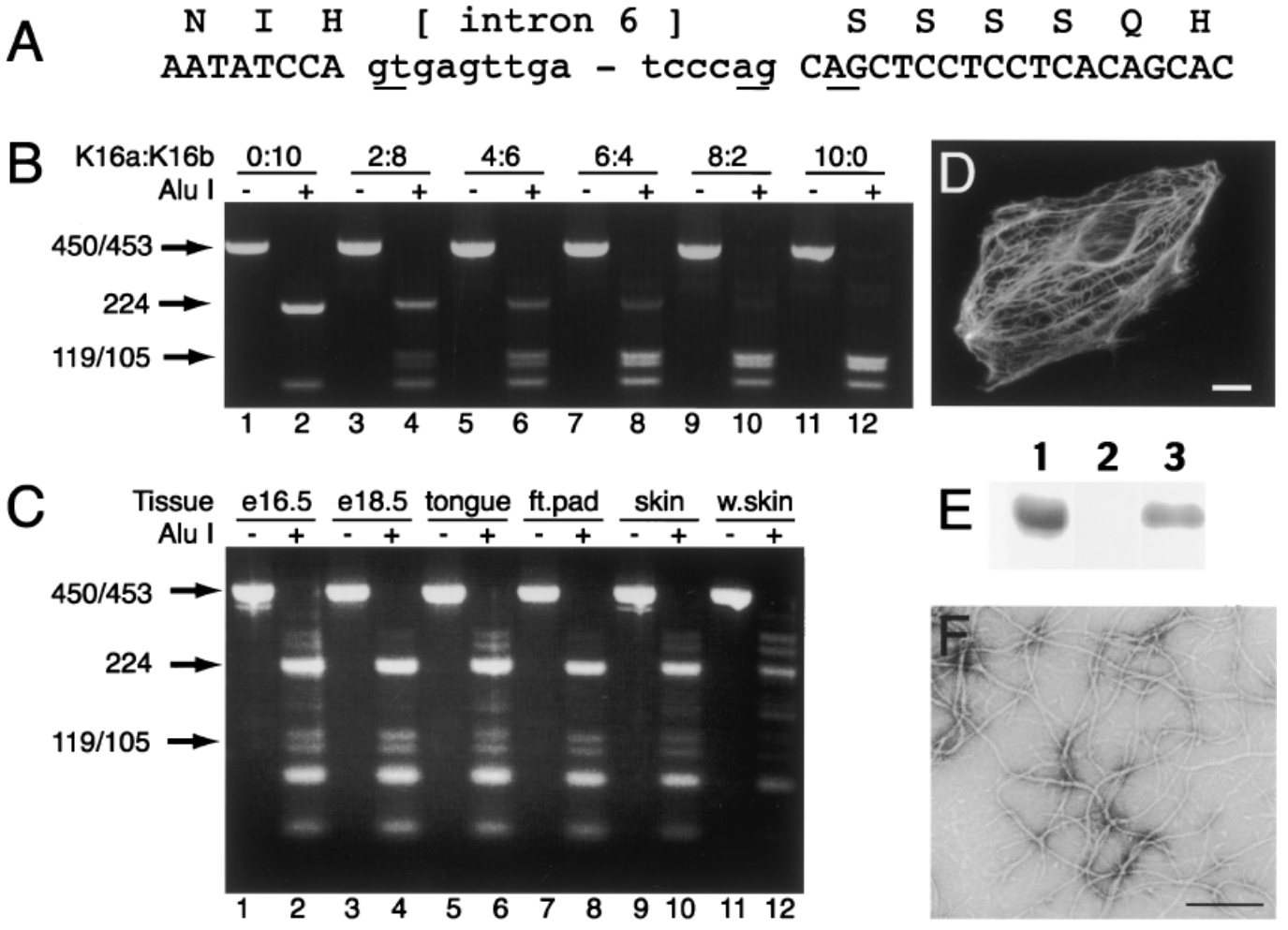

Figure 1. Cloning and expression of mouse K16. (*A*) The mouse K16 gene (GenBank Accession #AF24006) has two adjacent splice acceptor sites, AG, at the end of intron 6. Alternative use of the second site (mK16b) results in one less serine-encoding codon at amino acid position 406. The extra base pairs in mK16a create an additional Alu I restriction enzyme site, allowing for the identification of mK16a by RT-PCR followed by digestion with Alu I. (*B*) The cDNA clones corresponding to mK16a and mK16b were used as templates for testing the validity of the assay. The two clones were mixed at molar ratios (K16a : K16b) of 0 : 10 (*lanes 1, 2*); 2 : 8 (*lanes 3, 4*); 4 : 6 (*lanes 5, 6*); 6 : 4 (*lanes 7, 8*); 8 : 2 (*lanes 9, 10*); 10 : 0 (*lanes 11, 12*). Undigested (*odd-numbered lanes*) and Alu I-digested (*even-numbered lanes*) are shown. The K16b isoform gave rise to a specific band at 224 bp (*lane 2*), whereas digestion of the K16a form produced specific bands at 119 and 105 base pairs (*lane 12*). (C) RNA samples prepared from various K16-expressing tissues were tested for their K16 isoform expression patterns using the RT-PCR/restriction digest assay validated in (*B*). The samples were as follows (undigested, digested): e16.5 skin (*lanes 1, 2*); e18.5 skin (*lanes 3, 4*); adult mouse tongue (*lanes 5, 6*); adult mouse footpad (*lanes 7, 8*); adult mouse back skin (*lanes 9, 10*); adult mouse back skin 48 h after experimental wounding (*lanes 11, 12*). K16b was consistently the predominant isoform, although both isoforms were present. (*D*) Transient transfection of mK16 cDNA (either isoform) into PtK2 cells resulted in incorporation of the translated protein into the existing K8/K18 filament network, as evidenced by its recognition by indirect immunofluorescence with the KHmK16 antiserum. *Bar*: 5 μm. (*E*) A newly produced rabbit antiserum, KHmK16, was tested by Western blot, and recognized a band of approximately 50 kDa from mouse primary keratinocyte extract (*lane 1*) that comigrated with recombinant mouse K16 protein (either isoform) (*lane 3*). The antiserum was unable to bind the keratinocyte extract in the presence of the original peptide (*lane 2*). (*F*) When purified recombinant mK16 protein was mixed with mouse K6β protein and subjected to assembly buffer conditions *in vitro*, the keratins were capable of forming 10 nm wide filaments. The micrograph is a negative stain of the filaments examined by transmission electron microscopy. *Bar*: 125 nm.

preincubated with the peptide used to generate the antibody (**Fig 1*E***). After purification of recombinant mouse K16 protein and its presumed partner K6, we combined the type I and type II keratins in a 1 : 1 molar ratio, purified the heterotypic complexes, and performed a filament assembly reaction. Recombinant K6 and K16 are capable of copolymerizing into filaments under various conditions (**Fig 1*F***).

K16 is expressed in adult epithelial appendages We analyzed the distribution of K16 in adult mouse epithelia using Bouin's-fixed, paraffin-embedded tissues. We found a distribution pattern almost identical to that previously reported for human K16 (Moll *et al*, 1982). In normal hairy skin, the mouse K16 antigen(s) is not found in interfollicular epidermis, except for rare, sporadic cells located in the lowermost suprabasal layer (**Fig 2*A***). K16 is expressed constitutively in many epithelial appendages, however. K16 is present in multiple layers of the outer root sheath (ORS) in the large vibrissae follicles (**Fig 2*B***) but appears to be restricted to the companion layer within pelage follicles (**Fig 2*D***). We detect K16 antigen(s) in the proximal nail fold and nail bed, but not the nail matrix or nail plate (**Fig 2*C***). In oral epithelia, K16 is detected in the anterior compartment and buttress column of the filiform papillae of dorsal tongue epithelium (**Fig 2*E***) and also in suprabasal cells of the upper and lower palate. Interestingly, we also find K16 immunoreactivity in penile spines (**Fig 4*F*, *F′***), an epithelial appendage found in many rodents, primates, and other mammals, but not humans. These spines are androgen-dependent and are thought to affect copulatory behavior (Dixson, 1991). Like

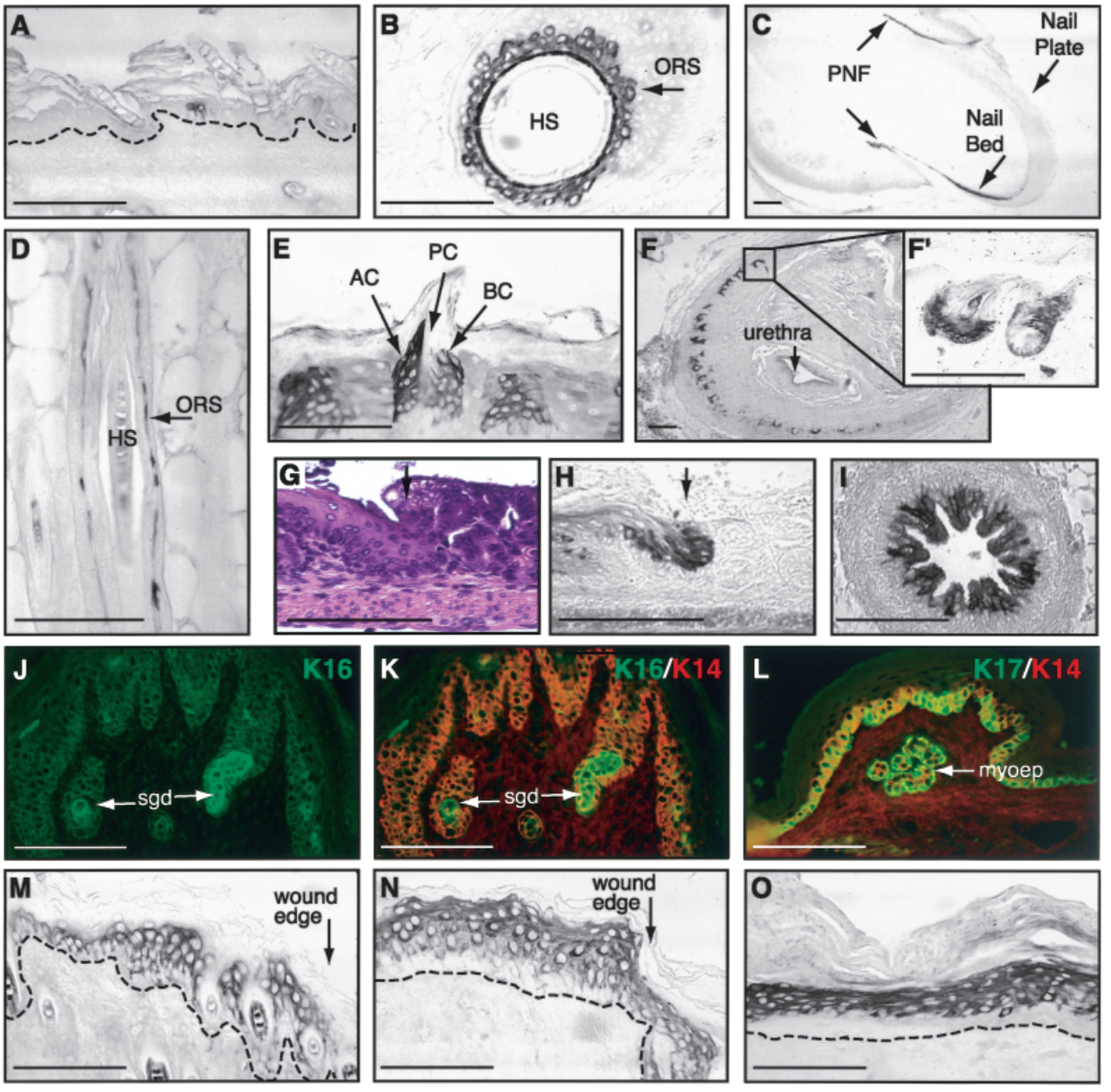

Figure 2. K16 detection in adult mouse tissue. Except where noted, all tissue sections were processed for immunohistochemistry with KHmK16 antiserum. (*A*) Normal adult skin; (*B*) vibrissa follicle in cross-section; (*C*) nail; (*D*) pelage hair follicle in longitudinal section; (*E*) tongue filiform papillae; (*F*) cross-section of penis; (*F′*) enlargement of penile spine; (*G*) hematoxylin and eosin stain of the stratified-squamous/simple-columnar epithelial junction in the forestomach; (*H*) serial section of (*G*), processed for K16 antigen; (*I*) ureter; (*J*) sweat glands in the foot pad; (*K*) same as (*J*), processed for double immunofluorescence of K14 and K16; (*L*) footpad and sweat glands, processed for double immunofluorescence of K14 and K17; (*M*) adult skin at 6 h after full-thickness injury; (*N*) adult skin at 48 h after full-thickness injury; (*O*) adult skin after series of treatments with retinoic acid. Dotted line indicates the dermal–epidermal junction where applicable. *Arrows*on (*M*) and (*N*) indicate the wound edge. HS, hair shaft; PNF, proximal nail fold; AC, anterior compartment; PC, posterior compartment; BC, buttress column; sgd, sweat gland duct; myoep, myoepithelium. *Scale bars*: 100 μm.

K6, K16 is present in the innermost layer of sweat gland ducts (**Fig 2*J***), whereas K14 (a related type I keratin) is in both layers of the duct (**Fig 2*K***). K16 is not found in myoepithelia as K17 and K14 are (**Fig 2*L***). In glabrous skin such as the foot pads, we observe K16 immunoreactivity in some basal and suprabasal cells (data not shown). In addition, expression of K16 is markedly induced in suprabasal cells after wounding of the skin (**Fig 2*M***, ***N***), or topical application of retinoic acid (**Fig 2*O***) or the phorbol ester PMA (see **Fig 7*E***). Mouse K16 is also expressed in internal stratified epithelia, such as the esophagus and vagina, and at the transition from stratified squamous epithelia to glandular epithelia in the forestomach (**Fig 4*G***, ***H***), anal canal, and nasal cavity. We also find K16 immunoreactivity in the transitional epithelia of the ureter (**Fig 4*I***), bladder, and urethra. Finally, there is patchy immunoreactivity in the medulla of the thymus.

K16 distribution during the hair cycle Because the first two hair cycles are synchronized in mouse, we are able to obtain skin sections with hair follicles at specific stages of the hair cycle. The K16 antigen is detected in the companion layer (the innermost layer) of the ORS of anagen stages III–VI (morphologically staged according to Muller-Rover *et al*, 2001). Because the companion layer of the ORS is composed of a single layer of very thin, flattened cells, only larger follicles with a favorable sectioning plane clearly demonstrate K16 immunoreactivity

(**Fig 3*B*, *C***). The use of unfixed frozen sections confirms that the K16 antigen is indeed present in the ORS of all hair follicles (data not shown). Intriguingly, we detect immunoreactivity of our mouse K16 antiserum in the hair shaft itself. We have previously determined that K17 is present in both the matrix and the medulla of the hair shaft (McGowan and Coulombe, 2000). To confirm that K16 is also in the hair shaft, we clipped hair from mice and performed two-dimensional gel electrophoresis followed by Western blotting (**Fig 3*F***). The spots recognized by our K16 antibody migrate at a position similar to the type I soft epithelial keratins and do not colocalize with type I hair keratins, which are smaller and more acidic than K16 (Lynch *et al*, 1986). The putative K16-containing spots are also recognized by the mouse monoclonal antibody K8.12, known to react with a different epitope shared by K13, K15, K16, and some hair keratins. The above evidence suggests that K16 protein is indeed found in the hair shaft.

As the hair follicle regresses towards the surface of the skin during catagen phase, K16 (as well as K6 and K17) localizes to the CHS (**Fig 4**), the layer of cells responsible for anchoring the club hair to the remaining ORS (Koch *et al*, 1998). K16 remains present during catagen V–VIII and most of telogen. Of note, K16 immunoreactivity within the CHS is easily detected in almost all hair follicles, in contrast to the ORS staining of anagen follicles.

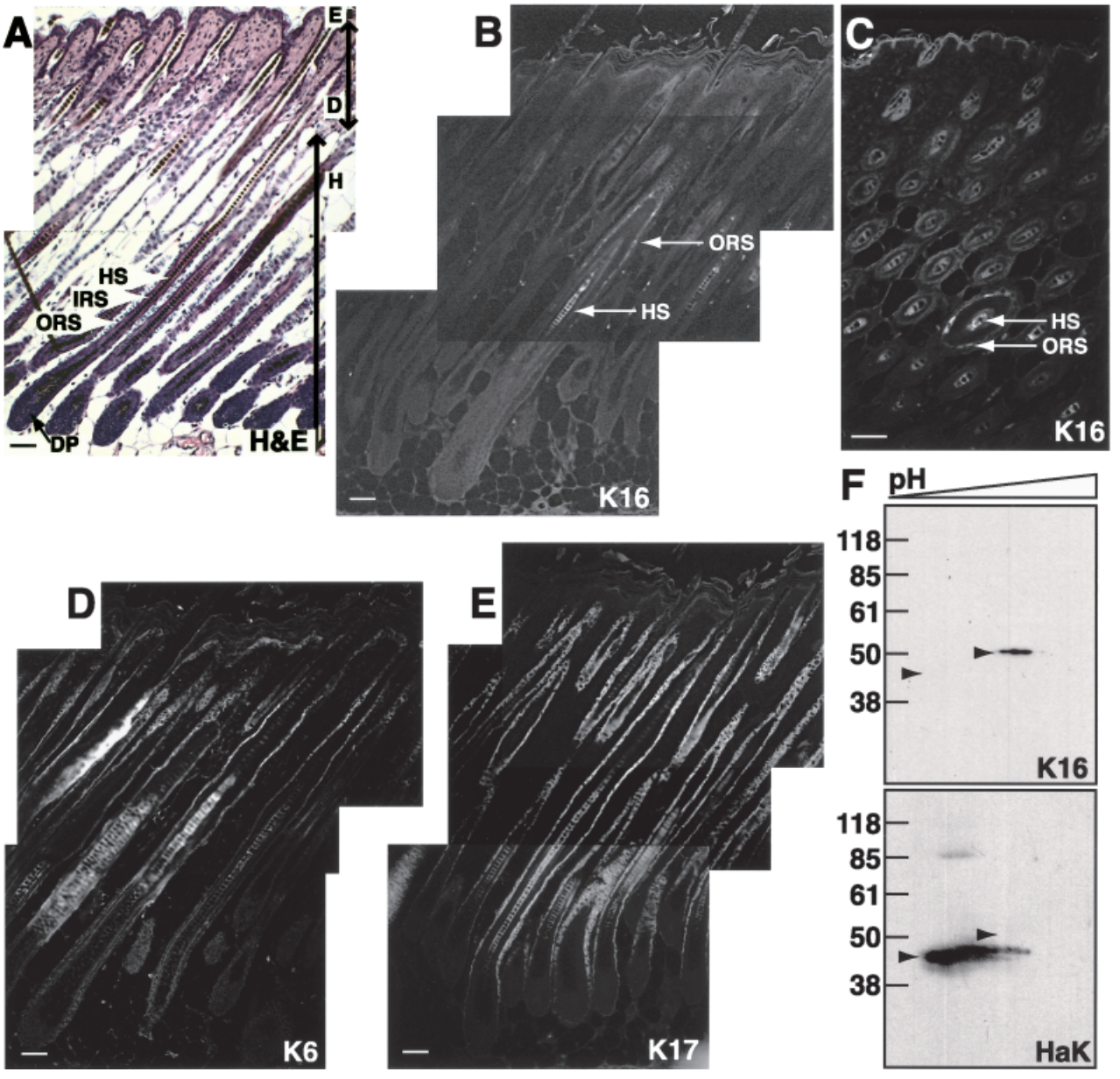

Figure 3. K6, K16, and K17 are present in the outer root sheath and the hair shaft during anagen. All sections were taken from dorsal skin of a 10-d-old pup, fixed in Bouin's, embedded in paraffin, and sectioned at 5 μm. (*A*) Hematoxylin and eosin stain; (*B*) K16 longitudinal sagittal section; K16 antigen was found in the companion layer of the ORS and the hair shaft. Not all follicles in the micrograph show reaction with our antiserum; however, the use of unfixed frozen sections confirmed antigen reactivity with all follicles. (*C*) K16 in cross-section. (*D*) K6 exhibits the same pattern as K16 in the ORS. In this instance, however, hair shaft staining was not confirmed by two-dimensional analysis. (*E*) K17 is expressed in all layers of the ORS (as opposed to just the companion layer) as well as in the hair shaft. (*F*) Protein from mouse pelage hair clippings was separated by two-dimensional gel electrophoresis followed by Western blot to demonstrate the presence of K16 in the hard epithelia of the hair shaft. *Arrowheads*are placed in identical positions in each blot. Note that our antibody does not cross-react with type I hair keratins (HaK), which are smaller and more acidic than K16. HS, hair shaft; IRS, inner root sheath; DP, dermal papilla; E, epidermis; d, dermis; H, hypodermis; ORS, outer root sheath. *Scale bars*: 50 μm.

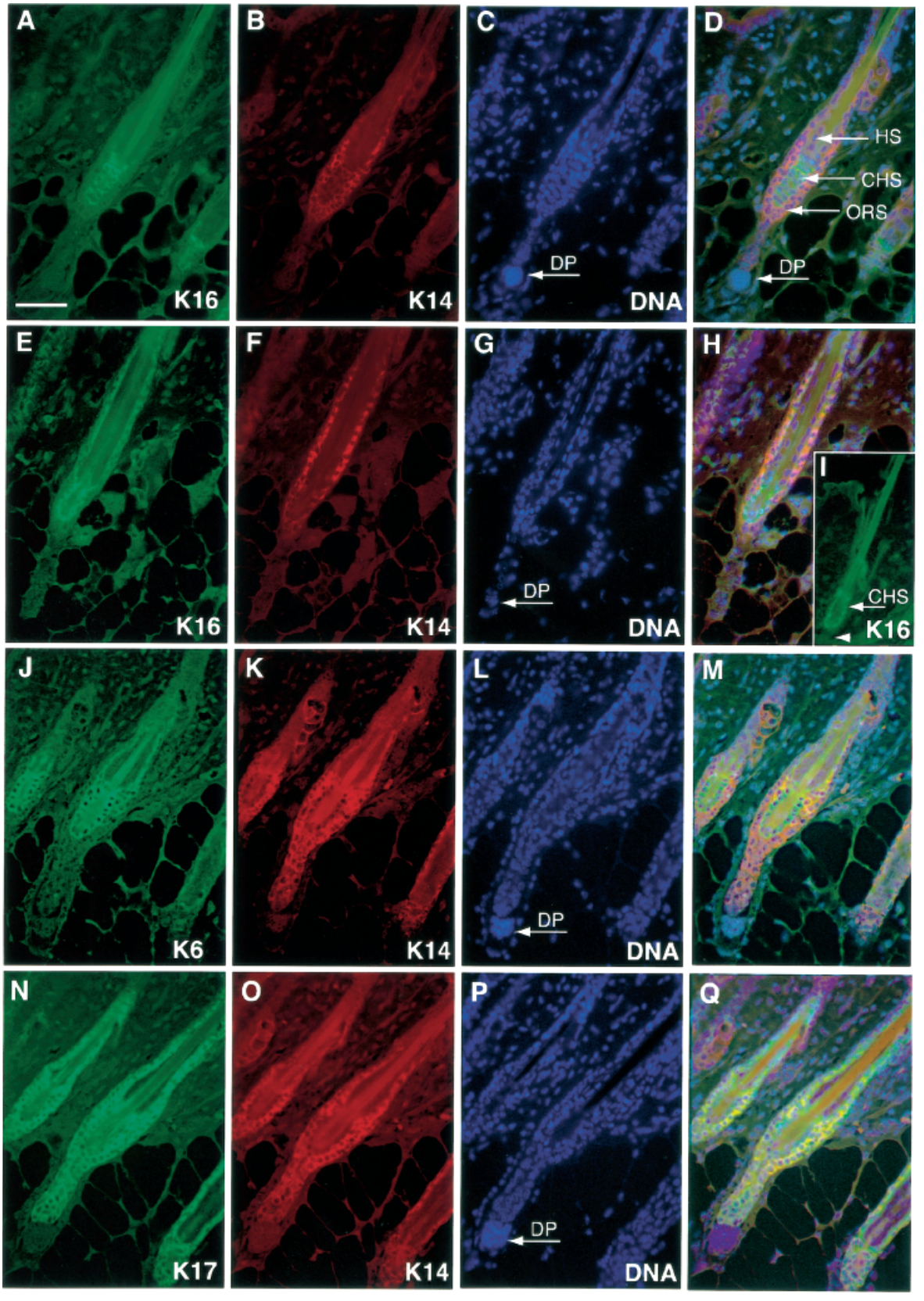

Figure 4. K6, K16, and K17 are present in the club hair sheath during catagen and telogen. All sections (except I) were from 18-d-old mouse dorsal skin that was fixed in Bouin's, embedded in paraffin, and sectioned. The antigen detected is listed in the lower right corner of each micrograph. Hoechst dye 33258 was used to stain the DNA in nuclei. (*D*), (*H*), (*M*), and (*Q*) are overlays of the other three micrographs in each row. (*I*) is a telogen follicle from a 25-d-old mouse immunostained for K16 to show the hair shaft and the CHS remain in this stage, although every cell in the CHS is no longer K16 positive. DP, dermal papilla; HS, hair shaft; ORS, outer root sheath; CHS, club hair sheath. *Scale bar*: 50 μm.

Electron microscopy shows the CHS cells to be morphologically distinct from the cells of the anagen-stage ORS in that they are more cuboidal in shape than the flattened cells of the companion layer (Lavker *et al*, 1998). K6, K16, and K17 immunoreactivity disappears near the telogen–anagen transition; every cell within the CHS no longer reacts with antisera against any of these three proteins. Once the second hair cycle has reached full anagen again, K16 immunoreactivity is detected in the companion layer of the ORS and the hair shaft itself.

K16 localizes within early hair follicle germs We obtained unfixed frozen mouse embryo sections ranging from e10.5 through birth, in 2 d increments. Using the KHmK16 antiserum, immunoreactivity with the K16 antigen is first detected at e12.5 (**Fig 5*A***). We observed only one group of cells showing immunoreactivity after serial sectioning through 300 μm of sagittal sections. This group of cells was located in the dorsal, posterior portion of the embryonic ectoderm. At e14.5, K16 immunoreactivity initially localizes to the majority of cells within the hair germ (stage 1 according to Paus *et al*, 1999) (**Fig 5*B–E***). Because maturation of skin appendages occurs in an anterior-to-posterior direction along the dorsal surface (Mann, 1962), multiple stages of hair follicle development can be seen by sampling along the entire dorsum of the embryo. As the hair germ elongates (stage 2), the distribution of K16 is seen to change in two ways. First, K16-intense cells appear more frequently in the center of the hair germ than along the outer edges. Second, K16-immunoreactive cells shift to a suprabasal location, above the hair germ and in the surrounding epidermis (**Fig 5*F–G***). As the hair germ evolves into a hair peg (stage 3), K16 is restricted to suprabasal cells in the vicinity of the developing hair follicle (**Fig 5*H***) until the formation of the ORS, at which time a favorable sectioning plane shows that some follicles are expressing K16 in the ORS (**Fig 5*I***). K16 localization in suprabasal cells of the epidermis continues to expand above and around the follicles. Within a few days after birth, however, K16 immunostaining disappears from interfollicular epidermis.

K16 expression is uncoupled from its presumed polymerization partner K6 Dual immunofluorescence was performed in order to better define the cells in which K16 is expressed in developing skin. **Figure 6(*A*)**, (***B***) shows that the K16 antigen is found to overlap both basal and suprabasal compartments; K16 partially colocalizes with both K14 (basal) and K10 (suprabasal). In addition, K16 is expressed in only a subset of K17-positive cells, a known marker of cells making the commitment to form a skin appendage (**Fig 6*C***) (McGowan and Coulombe, 1998a). Most surprising is the uncoupling of K16 expression from that of its presumed polymerization partner in adult epithelia, K6 (**Fig 6*D***). K6 and K17 are expressed in the outermost layer of the embryo, the periderm, which is shed before birth. We are unable to detect K16 antigen in the periderm except for the very rare cell (perhaps one or two cells per 5 μm thick whole embryo sagittal cross-section). This finding differs from human fetal periderm, where both K6 and K16 are expressed (Swensson *et al*, 1998). We cannot exclude the possibility that K16 is present in mouse periderm but not observed in the majority of cells due to antigen masking. K6 and K16 are also uncoupled in the hair germ. It should be noted that there are two isoforms of K6 (K6α and K6β; Takahashi *et al*, 1998) and an additional K6-related sequence, designated K6hf

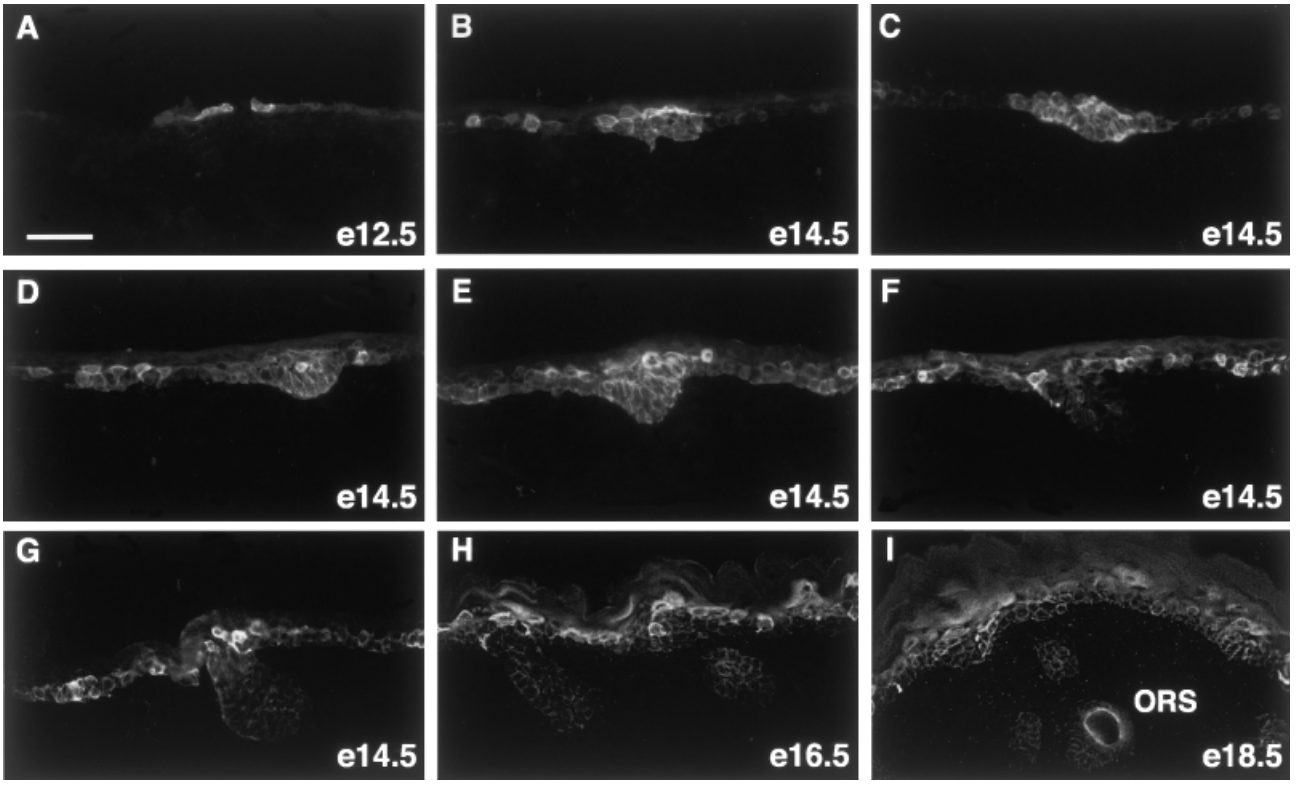

Figure 5. Mouse K16 during hair follicle morphogenesis. The KHmK16 antiserum was applied to frozen sections taken from mouse embryos at various stages of embryonic development. (*A*) At e12.5, K16 immunoreactivity was observed in a single patch of cells. (*B*)–(*G*) Because hair follicle maturation occurs in a wave of progression along the anterior-posterior axis, multiple stages of hair follicle morphogenesis can be observed by sampling along the dorsum of e14.5 embryos. (*B*)–(*E*) In stage 1 follicles, K16 localized to almost all cells within the hair germ. (*F*)–(*G*) As the germ elongated into stage 2, K16 immunoreactivity shifted towards cells above and around the germ and also towards the center of the germ (better seen in **Fig 6**). (*H*) K16 disappeared from the hair peg by the time it reached stage 3; instead, K16 localized in a patchy fashion to the bottom-most cells of the suprabasal layers at e16.5. (*I*) By e18.5, K16 was detected in the outer root sheath of follicles with a favorable sectioning plane. *Bar*: 50 μm.

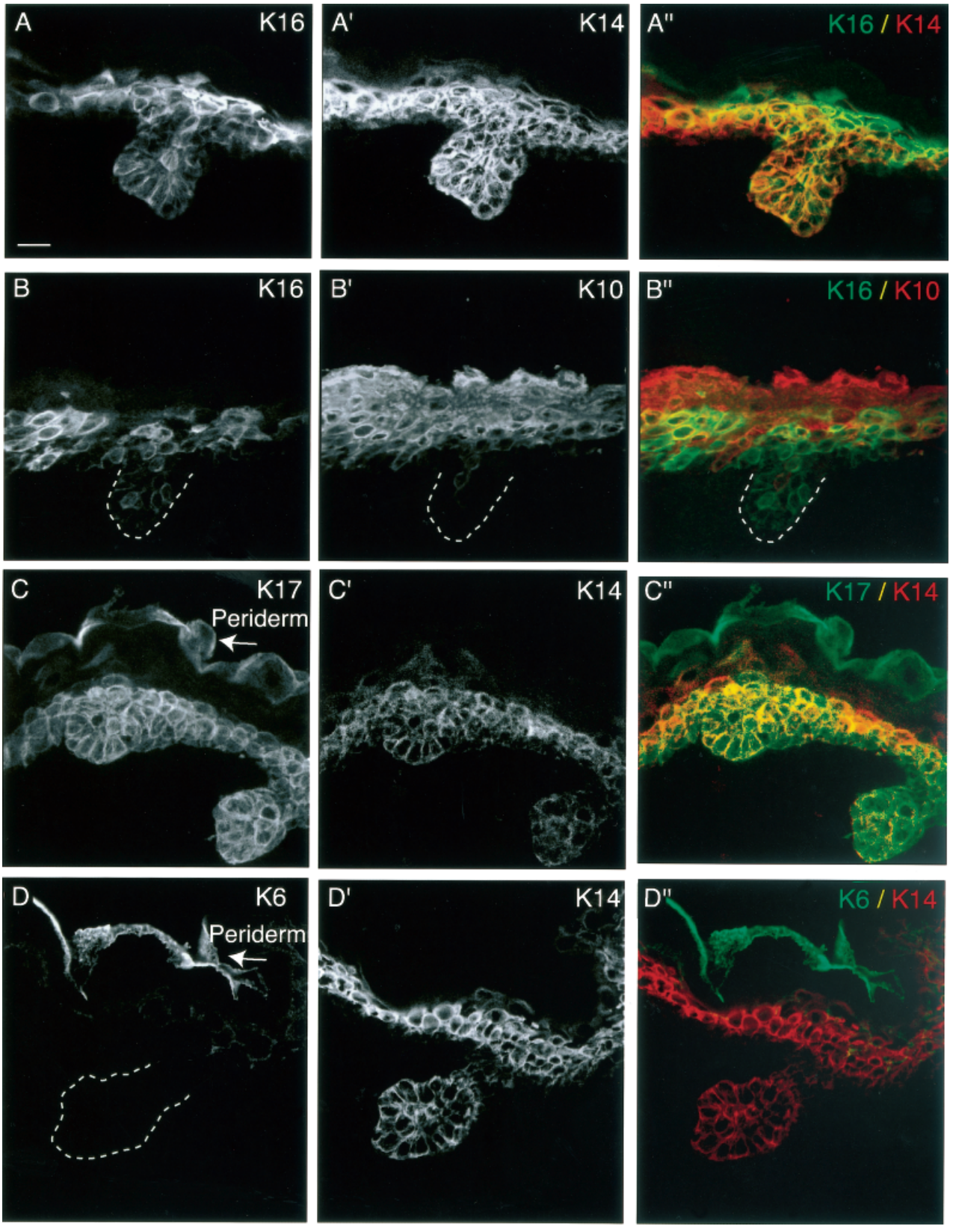

Figure 6. K16 localization is uncoupled from other keratins including its presumed polymerization partner, K6. Frozen e16.5 embryos were sectioned and processed for double indirect immunofluorescence. The micrographs were taken with a confocal scanning microscope. Each row represents the same hair germ. The double prime designation (*X″*) corresponds to the overlay of the two individual signals. (*Series A*) K16 antigen partially colocalized with K14, a marker for basal, mitotically active cells. The K16-positive cells were in the uppermost portion of the K14-positive cells. Note also the K16-bright cell in the center of the follicle. (*Series B*) K16 antigen colocalized with a subset of K10-positive cells present in the lowermost layer of the suprabasal cells. K10 is a marker for suprabasal cells that have entered the pathway for terminal differentiation. (*Series C*) K17 colocalizes with K14 in the basal layer and is also present in the periderm. (*Series D*) K6 is expressed in the periderm, but is completely absent from developing hair follicles at this time. *Bar.* 20 μm.

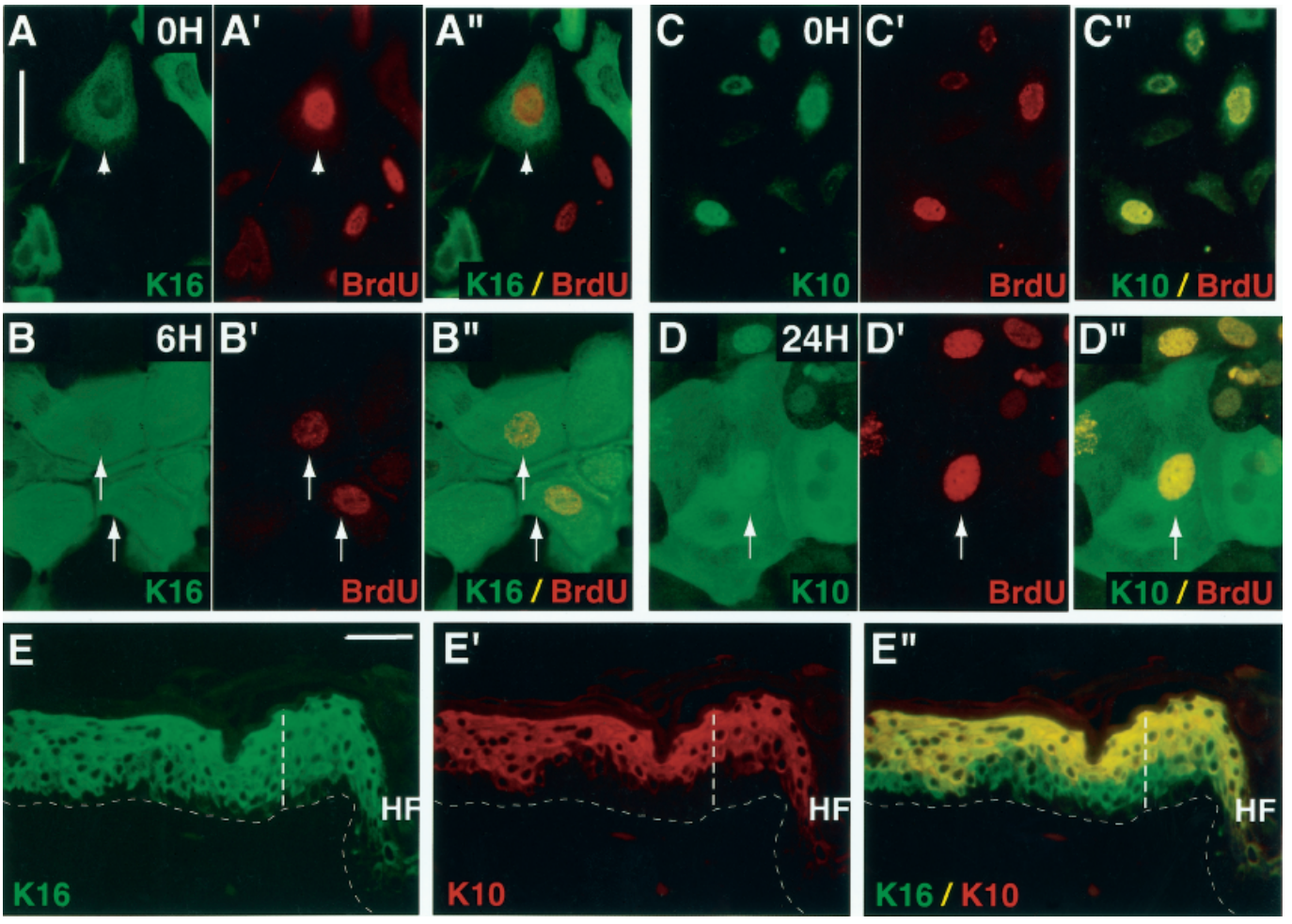

Figure 7. K16 marks an intermediate state of differentiation. (*A*)–(*D*) Primary keratinocytes were cultured in low-calcium, proliferation-inducing medium to 90% confluence, subjected to BrdU pulse, and then chased with high-calcium, differentiation-inducing medium. (*A*) K16 was heterogeneously induced in some cells in the low-calcium, proliferation-inducing medium. K16 immunoreactivity was seen only rarely in BrdU+ cells at this timepoint, however, and was usually dim compared to other cells. (*B*) K16+/BrdU+ cells were frequently seen after 6 h in differentiation-inducing medium. These cells demonstrated intense K16 immunoreactivity and exhibited morphological changes attributed to differentiating keratinocytes. (*C*) No K10+ cells were found at 0 h. Because the K10 and BrdU antibodies are both monoclonal, there was cross-reactivity of both secondary antibodies to BrdU+ nuclei. Note, however, that there was no filamentous or cytoplasmic staining at this timepoint. (*D*) K10+/BrdU+ cells were not seen until 24 h in the high-calcium, differentiation-inducing medium. Here, there was still cross-reactivity of the K10 secondary antibody to the BrdU+ nuclei, but filamentous keratin staining is obvious for K10. (*E*) Mouse back skin was treated with PMA to induce hyperproliferation. The tissue was processed for dual immunohistochemistry using antibodies for K16 and K10. Dashes on the vertical line represent approximate cell layers. The horizontal dashed line marks the bottom of the basal layer. K16 was found in the first two layers above the basal layer, whereas K10 was not found until three or four layers above the basal cell layer. *Scale bars*: 50 μm.

(Wojcik *et al*, 2001). None of the three keratins is found in the developing hair follicle until onset of lineage-specific gene expression such as hard keratins, filaggrin, and loricrin (Byrne *et al*, 1994; McGowan and Coulombe, 1998a; Rothnagel *et al*, 1999; Wojcik *et al*, 2001). Collectively these studies establish that, unlike the situation in adult epithelia, the regulation of K16 is uncoupled from that of K6 isoforms during the morphogenesis and differentiation of skin epithelia.

K16 expression may reflect an intermediate state of differentiation To investigate whether there are circumstances in which expression of K16 precedes that of K10 as part of epidermal differentiation in the adult, we conducted two types of studies. First, we performed a BrdU pulse-chase assay on keratinocytes in primary culture. Skin keratinocytes obtained from 3- to 5-d-old pups were cultured to 95% confluency in low-calcium, proliferation-inducing medium. During the last 2 h of growth in low-calcium medium, the cells were pulsed with BrdU. We then chased the BrdU label by incubating the cells in high-calcium medium to induce differentiation (Hennings *et al*, 1980; Yuspa *et al*, 1989). It has been shown that ^{3}H-thymidine incorporation is reduced by 25%, 90%, and >99% at 12, 24, and 36 h, respectively, after the addition of 1.2 mM calcium to mouse keratinocytes (Hennings *et al*, 1980). Moreover, morphological changes typically associated with differentiation, such as desmosome formation and closer apposition of neighboring cells, begin within 15 min of exposure to high calcium and are complete after 2 h (Hennings *et al*, 1980). Under the conditions of our assay, the BrdU signal diminishes in intensity if the cells continue to divide during the chase. On the other hand, a strong BrdU signal is retained throughout the chase (up to 96 h) if its incorporation took place during the last round of mitosis before onset of terminal differentiation. By performing dual immunohistochemistry with antibodies to BrdU and either K16 or K10, we were able to monitor the expression of these keratins during differentiation. The results obtained were as follows. Because K16 is heterogeneously expressed in cultured skin keratinocytes, we did see occasional K16+/BrdU+ cells at the 0 h timepoint; however, these double-positive cells had a weak signal for K16

(**Fig 7*A***). In contrast, we saw a marked increase both in K16 immunoreactivity and in the number of K16+/BrdU+ cells after just 6 h in the high calcium, differentiation-inducing medium (**Fig 7*B***). Unlike K16, K10 was not found in cells at the 0 h timepoint (**Fig 7*C***); in fact, we did not see K10+/BrdU+ cells until 24 h in the high calcium, differentiation-inducing medium (**Fig 7*D***). The antigens for K16 and K10 remained strong in signal throughout the course of the experiment due to the stability of these proteins. At the termination of the experiment, almost all keratinocytes were K16+, whereas only a subset of the K16+ cells were also K10+. We did not find any K10+/K16− cells. This experiment demonstrates that K16 is strongly induced prior to K10 in primary culture cells transitioning from mitosis to terminal differentiation.

In the second experiment, mouse back skin was treated with the phorbol ester PMA every other day over 6 d to induce hyperproliferation. Indirect immunohistochemistry of skin tissue harvested on the seventh day demonstrated that K16 immunoreactivity occurred in the first two or three cell layers above the basal layer, whereas K10 was not present until three or four cell layers above the basal layer (**Fig 7*E***). These studies show that, as appears to be the case in developing skin, expression of K16 can occur transiently in postmitotic keratinocytes of adult epidermis.

DISCUSSION

In spite of significant gains in our understanding of K16 properties in recent years, the wide array of contexts in which K16 is found poses a unique challenge when one is attempting to understand the significance of its presence in epithelial cells and tissues. Specifically, the human K16 gene exhibits constitutive expression in skin appendages, and inducible expression following injury or other forms of acute challenge to the skin, or in the context of disease (reviewed in McGowan and Coulombe, 1998b). Whether K16 performs a similar function and imparts similar properties to keratinocytes expressing it, irrespective of the context, is a fundamental issue that remains unsolved. To explore it further, we cloned and characterized the mouse K16 gene, and determined the distribution of its protein product in embryonic and adult mouse tissues. These efforts yielded several novel findings. First, during the adult hair cycle K16 is present in the ORS during anagen and the CHS during catagen and telogen. Second, onset of K16 expression occurs at an early stage of skin morphogenesis and exhibits a unique distribution that may reflect a hitherto unappreciated stage of keratinocyte differentiation. In this context, K16 is uncoupled from its presumed polymerization partner, K6. Third, there are circumstances in adult skin, other than wound repair (Paladini *et al*, 1996), in which epidermal keratinocytes transiently express K16 after they exit the cell cycle and before they undergo conventional keratinization. These findings provide new insight into the significance of K16 expression.

K16 expression is uncoupled from both K17 and its presumed polymerization partner K6 during development Many type I and type II keratin genes are invariably regulated as a pair in epithelia, including K5–K14, K1–K10, and, until this report, K6–K16. Most keratins can copolymerize with any other keratin of the opposing type *in vitro* (Hatzfeld and Franke, 1985), however, and some of them demonstrate considerable promiscuity in regard to their assembly partner(s) *in vivo*. For example, K17 is believed to pair with K5 in the basal cells of the ORS, K6 in the suprabasal cells of the ORS, and K5/K7 in myoepithelia (McGowan and Coulombe, 1998a; Schon *et al*, 1999). The demonstration that the distribution of K16 is distinct from that of its presumed partner K6 during embryonic development represents a rare instance of uncoupling in the regulation of these two keratins. K16 protein is at least partially stable in the absence of K6 in vivo as is evidenced by its presence in K6α/β null mice (Wong *et al*, 2000; Wojcik *et al*, 2001). The only other known difference in expression between these two keratins occurs in the response of mouse epidermis to acute challenge, where K6α and K17 are induced in both basal and suprabasal layers whereas K6β and K16 induction is restricted to the suprabasal layers (Takahashi *et al*, 1998; Reichelt and Magin, 2002). K5 could act as a type II partner for K16 in early hair germs; however, we cannot rule out the existence of a yet-to-be identified type II keratin in this context. The newly described type II keratin K6hf, best analogous to K5 in primary structure, is expressed in the periderm but not in the primary hair germs (Wojcik *et al*, 2001). Of potential interest, the micromechanical properties of K5–K16 filament assemblies were recently shown to differ from those of the natural pairs K8–K18 and K5–K14 in an *in vitro* setting (Bousquet *et al*, 2001; Yamada *et al*, 2002). That K16 has properties that are at least partially distinct from K14 *in vivo* was also demonstrated in keratin replacement studies in transgenic mice (Paladini and Coulombe, 1999; Wawersik and Coulombe, 2000; Wawersik *et al*, 2001). Given these observations, we expect the functional properties of K16-containing filaments to be slightly different during embryonic development depending in part on the type II polymerization partner involved.

K16 and the CHS The distribution of K16 changes during the mouse hair cycle. As is the case in human hair, K16 is expressed in the companion layer of the ORS from approximately anagen III through early catagen. As catagen progresses, K16 localizes to the cells of the CHS, and remains there until telogen, when immunoreactivity decreases. What remains unclear is the origin of the cells making up the CHS during catagen and telogen stages, and the role of K16 in these cells. This specialized layer of cells is required to anchor the telogen club hair and prevent premature loss of the hair. Generation of desmoglein 3 null mice showed that loss of adherence between the ORS and the IRS results in premature shedding of the club hair and temporary balding of the mice during each telogen stage of the hair cycle (Koch *et al*, 1998). Lavker and colleagues proposed that PAI-2 (plasminogen activator inhibitor type 2), a serine protease inhibitor expressed in the single layer of cells of the CHS and also in the hair shaft itself, acts as an inhibitor of premature death during the terminal differentiation (Lavker *et al*, 1998). Indeed the cells of the companion layer of the ORS, in which K6, K16, and K17 are expressed, keratinize very late compared to the other layers (Ito, 1986), and cells of the CHS also remain viable and metabolically active (Lavker *et al*, 1998). Again, the role of K16 in this particular setting is unknown. An attractive possibility is that CHS cells must be resilient and yet deformable to accommodate local stress, generated in this instance by the bending of hair at the skin surface. Such properties have been postulated for the differentiating palmo/plantar keratinocytes expressing K16 (Swensson *et al*, 1998), and may occur as well in keratinocytes of the nail bed, which are rich in K6, K16, and K17 (De Berker *et al*, 2000; McGowan and Coulombe, 2000).

Could K16 expression reflect an intermediate state of cellular properties? A model that would potentially account for the significance of K16 expression in nearly all relevant epithelial settings stipulates that its presence reflects an intermediate state of cellular properties. In this state, keratinocytes display characteristics that are intermediate between those of transient-amplifying (i.e., mitotically active and K14-expressing) and terminally differentiating (i.e., K10-expressing) cells in terms or their malleability and mechanical resilience. A similar concept has been proposed by Swensson *et al* (1998) based on correlative evidence obtained from studies of the distribution of K16 in human palmoplantar skin. There, the authors propose that expression of K16 in the secondary ridges provides zones of flexibility in between the stiffer, K9-expressing primary ridges.

We argue that expression of K6/K16 (and, presumably, the presence of many other proteins whose genes exhibit a similar regulation) and the resulting "intermediate state" could occur in

two contexts: as an "end stage phenomenon", or, alternatively, as a transient state. Examples of end-stage contexts include the constitutive expression of K16 in epithelial appendages of the adult, e.g., the CHS of the telogen-stage hair follicles (this study), the nail bed epithelium (McGowan and Coulombe, 1998a; De Berker *et al*, 2000), and the filiform papillae of the tongue (Wong *et al*, 2000). Examples of contexts in which K16 expression is transient, and keratinocytes would eventually progress to "normal" terminal differentiation, include wound repair in adult skin (e.g., Mansbridge and Knapp, 1987; Paladini *et al*, 1996), skin development (this study), and adult epidermis under disease (e.g., psoriasis; Stoler *et al*, 1988; Han *et al*, 2001) and related circumstances (e.g., primary culture, Schermer *et al*, 1989). Rather than attempting to relate the significance of K6/K16 expression to a specific program of epithelial differentiation, it would seem both easier and more inclusive of the available data to conceive of the presence of K6/K16 as conferring special properties to individual keratinocytes.

The model of K16 as a marker of keratinocytes with "intermediate" properties makes specific, testable predictions. Less differentiated keratinocytes, such as those found in the basal layer of epidermis and expressing K5/K14 (in addition to small amounts of K15; Lloyd *et al*, 1995; Porter *et al*, 2000), should display significantly different viscoelastic properties than fully differentiated keratinocytes loaded with K1/K10 and K2e. Consistent with activities such as mitosis and migration, which require the ability to undergo dynamic shape changes on a relatively rapid time scale, basal cells should be relatively malleable and flexible. In contrast, terminally differentiated keratinocytes should display the rigidity and resilience expected of cells taking part in the building of an effective barrier at the skin surface. Acquisition of this resilience should come at the expense of the flexibility characteristic of basal cells. Expression of K6/K16 would reflect the need, under specific but variable circumstances, to display intermediate properties. Unlike K5/K14 and K1/K10, K6/K16 would provide enhanced resilience without entirely abrogating the flexibility required to deform on a dynamic time scale. Presumably, such mixed properties are needed by an activated keratinocyte migrating in a wound site, in a developing hair placode, in the CHS, and in a variety of other contexts. An attractive feature of this model is that it implies that part of the significance underlying the existence of so many keratin genes comes from adapting the role of keratin intermediate filaments as structural scaffolds to the specific needs of individual types of epithelial cells (Coulombe and Omary, 2002). Useful methods for the assessment of the viscoelastic properties of pure keratin polymers reconstituted *in vitro* (Yamada *et al*, 2002) or of keratinocytes in culture (Yamada *et al*, 2000) are available so that this model can be put to a test.

We would like to thank Dr. Irene Leigh and Dr. Tung-Tien Sun for use of their antibodies. We are grateful to Dr. Stacy Mazzalupo for critical reading of the manuscript and to Dr. David Elliot for help with preparation of figures. This work was supported by an NIAMS/NIH grant AR44232 to P.A. Coulombe and an NRSA fellowship CA-67513 to K.M. McGowan.

REFERENCES

Bessho Y, Nakanishi S, Nawa H: Glutamate receptor agonists enhance the expression of BDNF mRNA in cultured cerebellar granule cells. *Brain Res Mol Brain Res* 18:201–208, 1993

Bousquet O, Ma L, Yamada S, *et al*: The nonhelical tail domain of keratin 14 promotes filament bundling and enhances the mechanical properties of keratin intermediate filaments *in vitro*. *J Cell Biol* 155:747–754, 2001

Byrne C, Tainsky M, Fuchs E: Programming gene expression in developing epidermis. *Development* 120:2369–2383, 1994

Chase HB, Eaton GJ: The growth of hair follicles in waves. *Ann NY Acad Sci* 83:365–368, 1959

Chase HB, Rauch H, Smith VW: Critical stages of hair development and pigmentation in the mouse. *Physiol Zool* 24:1–8, 1951

Chen S, Anderson K, Moore MJ: Evidence for a linear search in bimolecular 3′ splice site AG selection. *Proc Natl Acad Sci USA* 97:593–598, 2000

Coulombe PA, Fuchs E: Elucidating the early stages of keratin filament assembly. *J Cell Biol* 111:153–169, 1990

Coulombe PA, McGowan KM: Morphogenesis of skin epithelia. In: Drubin D, ed *Cell Polarity: Frontiers in Molecular Biology*. Oxford: Oxford University Press, 2000 pp 285–313

Coulombe PA, Omary MB: 'Hard' and 'soft' principles defining the structure, function and regulation of keratin intermediate filaments. *Curr Opin Cell Biol* 14:110–122, 2002

Coulombe PA, Ma L, Yamada S, Wawersik M: Intermediate filaments at a glance. *J Cell Sci* 114:4345–4347, 2001

De Berker D, Wojnarowska F, Sviland L, Westgate GE, Dawber RPR, Leigh IM: Keratin expression in the normal nail unit: markers of regional differentiation. *Br J Dermatol* 142:89–96, 2000

Dixson AF: Penile spines affect copulatory behaviour in a primate (*Callithrix jacchus*). *Physiol Behav* 49:557–562, 1991

Dry F: Coat of the mouse (*mus musculus*). *J Genet* 16:287–340, 1926

Fuchs E, Cleveland DW: A structural scaffolding of intermediate filaments in health and disease. *Science* 279:514–519, 1998

Greer J, Roop D: Loricrin, a major keratinocyte cell envelope protein, is expressed late in development. *J Invest Dermatol* 96:553–560, 1991

Han KH, Huh CH, Cho KH: Proliferation and differentiation of the keratinocytes in hyperplastic epidermis overlying dermatofibroma: immunohistochemical characterization. *Am J Dermatopathol* 23:90–98, 2001

Hardman MJ, Sisi P, Banbury DN, Byrne C: Patterned acquisition of skin barrier function during development. *Development* 125:1541–1552, 1998

Hardy MH: The secret life of the hair follicle. *Tends Genet* 8:55–61, 1992

Hatzfeld M, Franke WW: Pair formation and promiscuity of cytokeratins: fo. *J Cell Biol* 101:1826–1841, 1985

Hennings H, Michael D, Cheng C, Steinert P, Holbrook K, Yuspa SH: Calcium regulation of growth and differentiation of mouse epidermal cells in culture. *Cell* 19:245–254, 1980

Hesse M, Franz T, Tamai Y, Taketo MM, Magin TM: Targeted deletion of keratins 18 and 19 leads to trophoblast fragility and early embryonic lethality. *Embo J* 19:5060–5070, 2000

Ito M: The innermost cell layer of the outer root sheath in anagen hair follicle: light and electron microscopic study. *Arch Dermatol Res* 279:112–119, 1986

Kaufman MH: *The Atlas of Mouse Development*. London: Academic Press, 1992

Koch PJ, Mahoney MG, Cotsarelis G, Rothenberger K, Lavker RM, Stanley JR: Desmoglein 3 anchors telogen hair in the follicle. *J Cell Sci* 111:2529–2537, 1998

Kopan R, Fuchs E: A new look into an old problem: keratins as tools to investigate determination, morphogenesis, and differentiation in skin. *Genes Dev* 3:1–15, 1989

Lavker RM, Risse B, Brown H, Ginsburg D, Pearson J, Baker MS, Jensen PJ: Localization of plasminogen activator inhibitor type 2 (PAI-2) in hair and nail: implications for terminal differentiation. *J Invest Dermatol* 110:917–922, 1998

Lloyd C, Yu QC, Cheng J, Turksen K, Degenstein L, Hutton E, Fuchs E: The basal keratin network of stratified squamous epithelia. Defining K15 function in the absence of K14. *J Cell Biol* 129:1329–1344, 1995

Lynch MH, O'Guin WM, Hardy C, Mak L, Sun TT: Acidic and basic hair/nail ('hard') keratins: their colocalization in upper cortical and cuticle cells of the human hair follicle and their relationship to 'soft' keratins. *J Cell Biol* 103:2593–2606, 1986

Mann SJ: Prenatal formation of hair follicle types. *Anat Rec* 144:135–142, 1962

Mansbridge JN, Knapp AM: Changes in keratinocyte maturation during wound healing. *J Invest Dermatol* 89:253–263, 1987

McGowan KM, Coulombe PA: Onset of keratin 17 expression coincides with the definition of major epithelial lineages during skin development. *J Cell Biol* 143:469–486, 1998a

McGowan KM, Coulombe PA: The wound repair associated keratins 6, 16, and 1: insights into the role of intermediate filaments in specifying cytoarchitecture. In: Harris JR, Herrmann H, eds. *Subcellular Biochemistry: Intermediate Filaments*. London: Plenum, 1998b: pp 141–165

McGowan KM, Coulombe PA: Keratin 17 expression in the hard epithelial context of the hair and nail, and its relevance for the pachyonychia congenita phenotype. *J Invest Dermatol* 114:1101–1107, 2000

Moll R, Franke WW, Schiller DL, Geiger B, Krepler R: The catalog of human cytokeratins: patterns of expression in normal epithelia, tumors and cultured cells. *Cell* 31:11–24, 1982

Muller-Rover S, Handjiski B, van der Veen C, *et al*: A comprehensive guide for the accurate classification of murine hair follicles in distinct hair cycle stages. *J Invest Dermatol* 117:3–15, 2001

O'Guin WM, Schermer A, Lynch M, Sun T-T: Differentiation-specific expression of keratin pairs. In: Goldman RD Steinert PM, eds. *Cellular and Molecular Biology of Intermediate Filaments*. Plenum, 1990: pp 301–334

Paladini RD, Coulombe PA: Directed expression of keratin 16 to the progenitor basal cells of transgenic mouse skin delays skin maturation. *J Cell Biol* 142: 1035–1051, 1998

Paladini RD, Coulombe PA: The functional diversity of epidermal keratins revealed by the partial rescue of the keratin 14 null phenotype by keratin 16. *J Cell Biol* 146:1185–1201, 1999

Paladini RD, Takahashi K, Gant TM, Coulombe PA: cDNA cloning and bacterial expression of the human type I keratin 16. *Biochem Biophys Res Comm* 215:517–523, 1995

Paladini RD, Takahashi K, Bravo NS, Coulombe PA: Onset of re-epithelialization after skin injury correlates with a reorganization of keratin filaments in wound edge keratinocytes: de. *J Cell Biol* 132:381–397, 1996

Paramio JM, Casanova ML, Segrelles C, Mittnacht S, Lane EB, Jorcano JL: Modulation of cell proliferation by cytokeratins K10 and K16. *Mol Cell Biol* 19:3086–3094, 1999

Paus R, Muller-Rover S, Van Der Veen C, *et al*: A comprehensive guide for the recognition and classification of distinct stages of hair follicle morphogenesis. *J Invest Dermatol* 113:523–532, 1999

Porter RM, Hutcheson AM, Rugg EL, Quinlan RA, Lane EB: cDNA cloning, expression, and assembly characteristics of mouse keratin 16. *J Biol Chem* 273:32265–32272, 1998

Porter RM, Lunny DP, Ogden PH, *et al*: K15 expression implies lateral differentiation within stratified epithelial basal cells. *Laboratory Invest* 80:1701–1710, 2000

Purkis PE, Steel JB, Mackenzie IC, Nathrath WB, Leigh IM, Lane EB: Antibody markers of basal cells in complex epithelia. *J Cell Sci* 97:39–50, 1990

Reichelt J, Magin TM: Hyperproliferation, induction of c-Myc and 14-3-3s, but no cell fragility in keratin-10-null mice. *J Cell Sci* 115:2639–2650, 2002

Rhouabhia M, Germain L, Belanger F, Guignard R, Auger FA: Optimization of murine keratinocyte culture for the production of graftable epidermal sheets. *J Dermatol* 19:325–334, 1992

Rosenberg M, RayChaudhury A, Shows TB, Le BM, Fuchs E: A group of type I keratin genes on human chromosome 17: characterization and expression. *Mol Cell Biol* 8:722–736, 1988

Rothnagel JA, Seki T, Ogo M, *et al*: The mouse keratin 6 isoforms are differentially expressed in the hair follicle, footpad, tongue, and activated epidermis. *Differentiation* 65:119–130, 1999

Sambrook J, Fritsch EF, Maniatis T: *Molecular Cloning: A Laboratory Manual*. Cold Spring Harbor, NY: Cold Spring Harbor Laboratory, 1989

Sanes JR, Rubenstein JLR, Nicolas J-F: Use of a recombinant retrovirus to study post-implantation cell lineage in mouse embryos. *EMBO J* 5:3133–3142, 1986

Schermer A, Jester JV, Hardy C, Milano D, Sun TT: Transient synthesis of K6 and K16 keratins in regenerating rabbit corneal epithelium: keratin markers for an alternative pathway of keratinocyte differentiation. *Differentiation* 42:103–110, 1989

Schon M, Benwood J, O'Connell-Willstaedt T, Rheinwald JG: Human sweat gland myoepithelial cells express a unique set of cytokeratins and reveal the potential for alternative epithelial and mesenchymal differentiation states in culture. *J Cell Sci* 112:1925–1936, 1999

Sengel P: Epidermal–dermal interactions during formation of skin and cutaneous appendages. In: Goldsmith AL, ed. *Biochemistry and Physiology of Skin*. New York: Oxford University Press, 1983

Stoler A, Kopan R, Duvic M, Fuchs E: Use of monospecific antisera and cRNA probes to localize the major changes in keratin expression during normal and abnormal epidermal differentiation. *J Cell Biol* 107:427–446, 1988

Swensson O, Langbein L, McMillan JR, *et al*: Specialized keratin expression pattern in human ridged skin as an adaptation to high physical stress. *Br J Dermatol* 139:767–775, 1998

Takahashi K, Folmer J, Coulombe PA: Increased expression of keratin 16 causes anomalies in cytoarchitecture and keratinization in transgenic mouse skin. *J Cell Biol* 127:505–520, 1994

Takahashi K, Yan B, Yamanishi K, Imamura S: PA: The two functional type II keratin 6 genes of mouse show a differential regulation and evolved independently from their human orthologs. *Genomics* 53:170–183, 1998

Troyanovsky SM, Leube RE, Franke WW: Characterization of the human gene encoding cytokeratin 17 and its expression pattern. *Eur J Cell Biol* 59:127–137, 1992

Wawersik M, Coulombe PA: Forced expression of keratin 16 alters the adhesion, differentiation, and migration of mouse skin keratinocytes. *Mol Biol Cell* 11: 3315–3327, 2000

Wawersik M, Paladini RD, Noensie E, Coulombe PA: A proline residue in the α-helical rod domain of type I keratin 16 destabilizes keratin heterotetramers and influences incorporation into filaments. *J Biol Chem* 272:32557–32565, 1997

Wawersik MJ, Mazzalupo S, Nguyen D, Coulombe PA: Increased levels of keratin 16 alter the epithelialization potential of skin keratinocytes *in vivo* and *ex vivo*. *Mol Biol Cell* 12:3439–3450, 2001

Weedon D, Strutton G: Apoptosis as the mechanism of the involution of hair follicles in catagen transformation. *Acta Derm Venereol* 61:335–339, 1981

Wojcik SM, Longley MA, Roop DR: Discovery of a novel murine keratin 6 (K6) isoform explains the absence of hair and nail defects in mice deficient for K6α and K6β. *J Cell Biol* 154:619–630, 2001

Wong P, Colucci-Guyon E, Takahashi K, Gu C, Babinet C, Coulombe PA: Introducing a null mutation in the mouse K6α and K6βgenes reveals their essential structural role in the oral mucosa. *J Cell Biol* 150:921–928, 2000

Yamada S, Wirtz D, Kuo SC: Mechanics of living cells measured by laser tracking microrheology. *Biophys J* 78:1736–1747, 2000

Yamada S, Wirtz D, Coulombe PA: Pairwise assembly determines the intrinsic potential for self-organization and mechanical properties of keratin filaments. *Mol Biol Cell* 13:382–391, 2002

Yuspa SH, Kilkenny AE, Steinert PM, Roop DR: Expression of murine epidermal differentiation markers is tightly regulated by restricted extracellular calcium concentrations *in vitro*. *J Cell Biol* 109:1207–1217, 1989